Sensors & Actuators: B. Chemical 410 (2024) 135673

Contents lists available at ScienceDirect

Sensors and Actuators: B. Chemical

journal homepage: www.elsevier.com/locate/snb

Genetically encoded red fluorescent pH ratiometric sensor: Application to measuring pH gradient abnormalities in cystic fibrosis cells

Rafael Salto [a,1], Maria D. Giron [a,2], Jose M. Paredes [b,3,*]

[a] Department of Biochemistry and Molecular Biology II, Faculty of Pharmacy, Unidad de Excelencia en Quimica Aplicada a Biomedicina y Medioambiente (UEQ), University of Granada, Granada 18071, Spain
[b] Nanoscopy-UGR Laboratory, Department of Physical Chemistry, Faculty of Pharmacy, Unidad de Excelencia en Quimica Aplicada a Biomedicina y Medioambiente (UEQ), University of Granada, Granada 18071, Spain

ARTICLE INFO

Keywords:
pH sensor
Red Fluorescent protein
Intracellular probes, Lysosomal pH gradient,
Cystic fibrosis, Lysosome-related diseases

ABSTRACT

Genetically encoded probes to measure in vivo pH are challenging. They must be chloride insensitive and require normalization of the transfection efficiency. Furthermore, probes that emit in the red or far red are advisable to promote in vivo use. The mBeRFP D162T fluorescent protein presents two emission bands with different pH sensitivities. When the probe was cytosolic-expressed in HeLa as control cells and CFBE41o, an epithelial cell line that carries an F508del mutation in the CFTR transporter, the ratiometric measurement between both emission bands allows us to determine the pH, demonstrating that mBeRFP D162T can be used to accurately measure the cytosolic pH differences of these cell lines.

Furthermore, we have located the sensor inside or outside the lysosomal membrane to investigate the lysosomal pH gradient. In HeLa cells, our probe detected pH gradient changes under conditions known to alter lysosomal pH. In the CFBE41o cells, which mimic cystic fibrosis disease, we observed a complete loss of lysosomal acidification. Using lumacaftor, a drug that restores functioning CFTR protein, partially brings back the pH gradient. In conclusion, mBeRFP D162T is a valuable tool for measuring in vivo intracellular pH values and lysosomal pH gradient dynamics in physiological or pathological conditions.

1. Introduction

pH sensors based on non-invasive methods, such as fluorescence microscopy, have been recognized as crucial tools. They provide exceptional sensitivity, user-friendly operation, and rapid response to the target analyte. Among fluorescent sensors, fluorescent proteins (FP) stand out as the most used probes for visualizing the spatiotemporal dynamics of cells[1,2]. These fluorophores are genetically encoded, thereby avoiding any complications associated with loading procedures and ensuring noninvasive imaging. Furthermore, FPs offer the advantage of selective targeting to particular cell types, specific intra/-extracellular locations or subcellular compartments by fusion with specific targeting signals[3]. Among the different strategies for measuring pH using FPs, ratiometric-based measurements depend on the changes in the intensity of two or more emission signals. Unlike sensors that rely on a single emission signal, ratiometric measurements can overcome limitations associated with gene expression level and photobleaching. Consequently, in sensors relying on a single emission signal, determining the absolute pH value based solely on changes in fluorescence intensity is not feasible. However, pH sensors based on ratiometric measurements can overcome such uncertainties by calculating the ratio of intensities at two different wavelengths[3]. Ratiometric sensors can be categorized based on either excitation or emission. In the first group, two different excitation wavelengths are utilized, typically resulting in one emission wavelength. Conversely, the second group employs a single excitation wavelength and two distinct emission

Abbreviations: FP, fluorescent proteins; FRET, Förster Resonance Energy Transfer; LSS, long Stokes shift; CF, Cystic fibrosis; CFTR, cystic fibrosis transmembrane conductance regulator transporter; ENaC, epithelial sodium channel.

* Corresponding author.
E-mail address: jmparedes@ugr.es (J.M. Paredes).
[1] orcid.org/0000-0002-7044-3611
[2] orcid.org/0000-0001-9638-988X
[3] orcid.org/0000-0002-3252-9174

https://doi.org/10.1016/j.snb.2024.135673
Received 11 August 2023; Received in revised form 26 January 2024; Accepted 19 March 2024
Available online 20 March 2024

wavelengths. Ratiometric measurements in pH sensors can be easily achieved by fusing two different FP[3,4]. This can be accomplished through Förster Resonance Energy Transfer (FRET)[5–7] or by fusing proteins with distinct pH sensitivities[7,8].

However, it is always preferred to have monomeric proteins in order to avoid size-related issues as aggregation. In literature, it can be found a few examples of single FPs that exhibit dual excitation[9,10] or emission with maxima in the blue/green region of the visible spectrum[11–13].

With the objective of expanding the color palette, mitigating background fluorescence, and enabling deep-tissue and whole-body experiments, multiple strategies have been developed to redshift the emission of FP variants[14,15]. The first redshifted ratiometric single FP pH sensor, pHRed[16], is based on dual excitation rather than dual emission.

In this study, we introduce a novel redshifted dual emission ratiometric single FP. This sensor is based on a red fluorescent protein from *Entacmaea quadricolor* and termed mBeRFP[17]. mBeRFP has a long Stokes shift (LSS) and constituted a flexible platform, where mutations can be introduced to enhance its properties as a biosensor. For example, the double mutant S94V, R205Y presents a high sensitivity to halide ions [18]. In this article we present a new mutation D162T that minimizes the sensitivity to halide ions. This modification helps to avoid signal interferences caused by fluctuations in chloride concentration. To the best of our knowledge, there are currently no described ratiometric single FP, chloride-independent, pH sensors based on dual emission.

Cystic fibrosis (CF) is the most prevalent monogenic recessive inherited disease in humans, where mutations in the cystic fibrosis transmembrane conductance regulator transporter (CFTR) hindrance its activity and are responsible for the disease[19]. The CFTR protein, in addition to its role as a chloride channel, is involved in various other functions. Among these functions, it participates in the bicarbonate ions (HCO_3^-) transport and regulates other transport channel as the epithelial sodium channel (ENaC)[20].

Early studies on CF identified that the alterations associated with the disease included changes in cell pH as well as defective acidification of intracellular organelles including lysosomes[21]. Albeit the contribution of CFTR to the acidification of the lysosome is not determined, the CFTR transporter is located at the lysosome membrane and its activation leads CFTR to the re-acidification of lysosomes from an elevated pH[22]. Furthermore, the lack of acidification in the lysosomes from CF patients' macrophages is relevant since is associated with a decreased bacterial clearance capability[23].

Considering the significance of acidification/alkalinization in cystic fibrosis[24], monitoring the real-time flux of pH inside living cells or organelles is essential. It enables the tracking of disease progression, evaluating treatment effectiveness, and investigation of new drugs aimed at minimizing these pH changes and, therefore, we have selected cells carrying mutations in the CFTR gene as a model to test the usefulness of the mBeRFP D162T protein to measure pH in the cytosol and lysosomes.

First, we assessed the capability of this new sensor to measure intracellular pH. Subsequently, we measured the pH gradient between the inner and outer membrane of lysosomes in two distinct cell types; HeLa and CFBE41o, a human cystic fibrosis bronchial epithelial cell line with the ΔF508 CFTR mutation. Lastly, we investigated the impact of two drugs (Lumacaftor[25] and CFTR(inh)-172[26]) on the pH gradient in this cell line.

2. Experimental section

2.1. Cloning and Site-directed mutagenesis

mBeRFP protein-encoding plasmid pRSET B-BeRFP[17], was kindly provided by Dr. Zhihong Zhang (Britton Chance Center for Biomedical Photonics, Wuhan National Laboratory for Optoelectronics, Huazhong University of Science and Technology, Wuhan, Hubei, China). Plasmid pBeRFP-C1 encodes for the eukaryotic expression of mBeRFP and, has been described previously [18]. Plasmid sfGFP-Lysosomes-20 was a gift from Michael Davidson (Addgene plasmid # 56487).

mBeRFP sequence has been PCR amplified from pBeRFP-C1 plasmid using the oligonucleotides $BeRFP_F$ and $BeRFP_{NotI}$ (see Supporting Information Table S1), which include an *Age*I and a *Not*I restriction site, respectively. The PCR product was cloned into the pJET 1.2 vector (Thermo Fisher Scientific, Madrid, Spain) and then digested with *Age*I-*Not*I to replace the sfGFP coding sequence in the sfGFP-Lysosomes-20 eukaryotic expression vector. The new plasmid was termed pLAMP1-mBeRFP (complete sequence in Supporting Information S2). By using this plasmid, mBeRFP is expressed at the cytosolic face of the lysosome membrane.

To generate a lysosomal expression vector for mBeRFP where the mBeRFP is located at the lysosomal membrane facing the matrix, first in a linker termed Lysnker that codified for a signal peptide sequence and *Nhe*I and *Age*I restriction sites (see Supporting Information Table S1), has been cloned in the pBeRFP-C1 plasmid to generate pSignal-BeRFP. Then, the LAMP1 coding sequence was amplified from sfGFP-Lysosomes-20 plasmid using the LampF and LampR oligonucleotides which include *Eco*RI and *Sal*I restriction sites. The PCR product was cloned into the pJET 1.2 vector and then digested with *Eco*RI-*Sal*I to be inserted in the pSignal-BeRFP-C1 plasmid generating the final construct termed pSignal-mBeRFP-LAMP1 (complete sequence in Supporting Information S2).

Site-directed mutagenesis of either pRSET B-BeRFP or pLAMP1-mBeRFP and pSignal-mBeRFP-LAMP1 plasmids was carried out as described previously [27] to introduce mutations in the BeRFP coding sequence. The oligonucleotides used for site-directed mutagenesis are also provided in Supporting Information Table S1. The sequences of the generated plasmids were confirmed by automatic sequencing with universal primers.

2.2. Recombinant protein expression and purification

Bacterial expression of BeRFP and its mutated versions was carried out as described previously [18]. In brief, BL21(pLys) competent cells were transformed with the pRSET B-BeRFP plasmid (or the mutated plasmids) and grown in LB broth with selection antibiotics at 37°C overnight without induction. Purification of the proteins, after the lysis of the bacterial pellets was carried out by IMAC chromatography using a HisTrap FF crude column (GE Healthcare Life Sciences, Chicago, IL, USA). Eluted proteins were concentrated and dialyzed with PBS, and the protein concentration was measured by the bicinchoninic acid (BCA) method. Protein purity was confirmed by SDS-PAGE (Supporting Information, Figure S1).

2.3. Cell culture and DNA transfection assays

Human cervix adenocarcinoma (HeLa, ATCC: CCL-2) cells were supplied by the Cell Culture Facility (University of Granada, Spain). Human CF Bronchial Epithelial (CFBE41o, SCC151) cells were purchased from Sigma-Aldrich, Madrid, Spain. CFBE41o were grown onto fibronectin/bovine serum albumin/collagen-coated flasks. HeLa and CFBE41o cells were grown at 37 °C in Dulbecco's modified Eagle's medium (DMEM) supplemented with 10% (v/v) fetal bovine serum (FBS), 2 mM glutamine, 100 U/mL penicillin, and 0.1 mg/mL streptomycin.

Before transfection, cells were seeded onto μ-Slide 8 Well Chambered Coverslips (Ibidi, Gräfelfing, Germany) at a density of 2× 105 cells/well for 24 h to reach a cell confluence of 80−90%. For transfection experiments, plasmids were mixed with LP2000 at room temperature for 20 min following manufacturer protocol. Cells were incubated with the polyplexes for 5 h. The transfection medium was then removed, and cells were further grown in DMEM plus 10% FBS for an additional period of 24 h. Transfected cells were used for fluorescence microscopy and image

analysis.

For mitophagy assays, CFBE41o cells were transfected either with pGFP-LC3 plasmid (kindly provided by Tamotsu Yoshimori, Addgene plasmid #21073) or pSignal-mBeRFP-D162T-LAMP1 and then labelled with mitoTracker deep red FM (Thermo Fisher Scientific, Madrid, Spain). Mitophagy was detected using standard colocalization protocols [28].

2.4. Cell permeabilization

Cells were seeded onto μ-Slide 8 Well Chambered Coverslips and incubated in their respective medium. On the day of the experiment, cells were washed with phosphate-buffered saline (PBS) and punctured by incubation for 15 min at 37 °C with 2 μg/mL α-toxin in permeabilization buffer (20 mM potassium MOPS, pH 7.0, 250 mM mannitol, 1 mM potassium ATP, 3 mM MgCl2, and 5 mM potassium glutathione). The cells were then washed with the corresponding buffer three times and analyzed by fluorescence microscopy.

Ammonium pulse protocol was used to produce an intracellular pH change. This protocol includes three buffers, recording solution, that contains NaCl 140 mM, H_2PO_4 2.5 mM, $MgSO_4$ 1 mM, $CaCl_2$ 1 mM, HEPES 10 mM and glucose 6 mM (pH7.3); the second buffer is NH_4^+ solution, obtaining by replacing in the recording solution 30 mM NaCl with an equimolar concentration of NH_4Cl; when $NH4^+$ ions are transported into the cell, they produce a rise in the intracellular pH. The last buffer is the bicarbonate solution, by replacing in the recording solution 30 mM NaCl by $NaHCO_3$. Once the culture media is changed back, including $NaHCO_3$ in the culture media, the pH lowers.

2.5. Spectroscopy analysis fluorescence microscopy and image analysis

Absorption spectra were recorded using a Lambda 650 UV−visible spectrophotometer (PerkinElmer, Waltham, MA). For fluorescence excitation and emission spectra, a microplate reader CLARIOstar Plus (BMG Labtech, Germany) was employed.

The pK_a values were obtained by analyzing the changes in maximum intensity (I) or ratios (R) at various pH values using the next fitting equation.

$$I(or \quad R) = \frac{F_B + F_A 10^{pK_a - pH}}{1 + 10^{pK_a - pH}} \tag{1}$$

F_A and F_B represent the plateau values for fluorescence intensity or ratios under acidic and basic conditions, respectively.

The fluorescence intensity (I) was analyzed using the next 1:1 binding equation to determine the dissociation constant (k_d) for chloride binding.

$$I = \frac{F_0 + F_1[Cl^-]/k_d}{1 + [Cl^-]/k_d} \tag{2}$$

The equation takes into account the chloride concentration ($[Cl^-]$) and the fluorescence signals at zero and infinite chloride concentrations, represented as F_0 and F_1, respectively.

Microscopy images for ratiometric mBeRFP D162T measurements were captured using an Abberior scanning microscope (Abberior Instruments GmbH, Göttingen, Germany) with a pulsed excitation laser of 450 nm (40 MHz). A UPlanSApo objective (1.4 NA, 100X) oil immersion was used for imaging. The pinhole size was consistently set to 1 Airy unit (AU) for all measurements. The collected fluorescence was split by a 560LP dichroic mirror and directed to two detectors: an avalanche-photodiode (APD) and a hybrid photomultiplier tube (HPMT). The fluorescence passed through 685/75 (Red channel) and 509/11 (Green channel) filters before reaching the APD and HPMT detectors, respectively. For colocalization studies using mBeRFP D162T and GFP we used pulsed excitation laser of 561 nm (40 MHz) and 485 nm (40 MHz), respectively. Lysotracker was employed with a pulsed excitation laser of 640 nm (40 MHz).

Image processing was conducted using *Fiji is just image j* software[29] using custom macros. Firstly, the raw images were imported, and a Gaussian smoothing function was applied with a standard deviation of 0.5 pixels. Next, a region of interest (ROI) was manually selected to create binary masks, assigning a value of 0 for the background and 1 for the cells or lysosomes. Both channels of the images were then multiplied by the ROI, resulting in images containing values only for the cells. Finally, the images were divided to obtain the ratiometric image, which allowed the assessment of the pH values based on the ratio between the red and green fluorescence intensities. This image processing approach enabled the accurate quantification and analysis of pH variations within the cells and the lysosomal compartments.

2.6. Statistical analysis

Results were expressed as means ± SEM, n=6. The box and whisker plots depicted the mean, the 25th/50th/75th percentiles, and the SEM. The statistical significance of variations was evaluated using one- or two-way ANOVA or the corresponding non-parametric test depending on the homoscedasticity test (Bartlett's test). Post hoc paired comparisons, using Tukey's test or Dunn's test, were performed to check for significantly different effects between all pairs of diets using the Origin Pro 8.5 software. A p-value <0.05 was considered significant.

3. Results and discussion

3.1. Chloride desensitization and photophysical characterization

In our previous work, we had studied the presence of a dual emission band observed in the mBeRFP mutants. We found that chloride ions produce varying degrees of quenching between these emission bands, allowing us to determine chloride levels in biological systems where the pH remains stable[18]. In this study, we present a novel system for pH determination utilizing the unique dual emission characteristics of these mutant variants. The presence of these two emission bands can be attributed to the cis-trans isomerization of the chromophore, which is induced by changes in pH, as previously demonstrated in other studies in mBeRFP precursors[30–32].

To obtain a robust pH value, it is crucial to eliminate the chloride dependence of the signal. In our previous work, our aim was to investigate the effect of different mutations on the chloride affinity of the probe. Here, we performed an opposite approach, in which we aimed to identify the mutation that would cause the loss of affinity for chloride ions. We detected that the position 162 is implicated in chloride sensitivity. Mutations at this position, like Ala or Thr, lead to reduced chloride sensitivity. This is likely attributed to the charge loss upon Ala insertion, impeding hydrogen bond formation, or the increased steric hindrance caused by methyl group of Thr. To overcome chloride interference, we have specially chosen a mBeRFP bearing the D162T mutation, which significantly reduces the sensitivity of the FP to chloride within the physiological pH range and under intracellular acidic conditions, in contrast to mBeRFP, which shows a pronounced chloride dependence in acidic medium. To explore the chloride dependence on the fluorescence in both proteins, we have performed a Stern Volmer representation in Fig. 1A. The Stern-Volmer plot provides a graphical representation of the quenching phenomenon. Our data compares the chloride effect on mBeRFP and mBeRFP D162T demonstrating that no response to chloride is observed throughout the pH range examined in mBeRFP D162T, as shown in Fig. 1A and B, where stable fluorescence intensity is observed even up to 500 mM of chloride. This selective loss of chloride affinity ensures that the FP's fluorescence response is mainly governed by changes in pH rather than fluctuations in chloride concentrations, making it an ideal candidate for accurately and specifically detecting intracellular pH changes enabling more accurate and reliable pH measurements.

Once confirmed the independence of fluorescence intensity of the

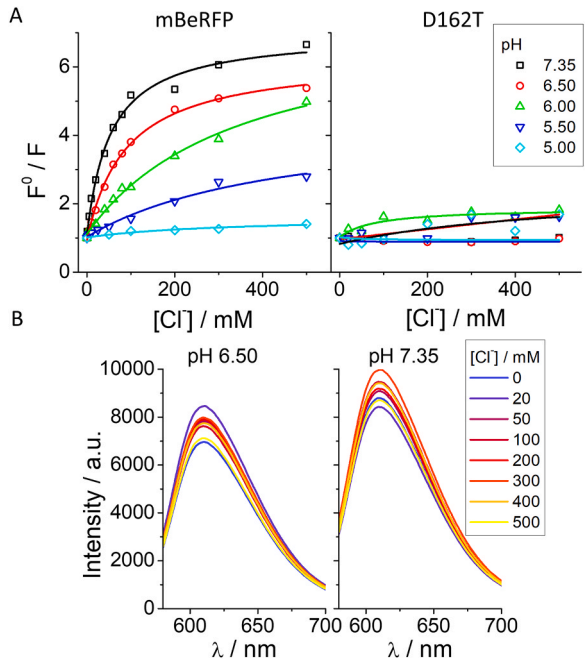

Fig. 1. Study of the independence of fluorescence emission with chloride. A) Left. Stern-Volmer representation showing the dependence of the mBeRFP concentration (λ_{ex}= 440 nm, λ_{em}=625 nm) (left) and mBeRFP D162T (λ_{ex} = 580 nm, λ_{em}=625 nm) (right) fluorescence intensity on chloride. Right. The curve is the fit of Eq. 2 to experimental data B) Fluorescence emission spectra of mBeRFP D162T (λ_{ex}= 580 nm) at pH 6.50 (left) and 7.35 (right) at different chloride concentrations.

mBeRFP D162T protein with respect to chloride ions, we proceeded to investigate the pH dependence of both emission bands. To accomplish this, we utilized two different excitation wavelengths (Supporting Information, Figure S2). Initially, we employed a wavelength of 580 nm to focus specifically on the species emitting only the red band, characterized by a maximum emission at 625 nm (see Fig. 2A). Consistent with other fluorescent proteins[11,16], we observed that the fluorescence intensity exhibited a pH-dependent behavior, showing an increase in intensity as the pH increased. This variation in the intensity of the redshifted emission is caused by the protonation of the chromophore. We studied the pK_a of the chemical equilibrium between the protonated and deprotonated forms of the chromophore. Our findings revealed a pK_a value of 5.72 ± 0.06, as shown in Fig. 2B. This value is appropriate since it provides a wide range that covers the entire spectrum of pH values found within the cell. Moreover, the sensor exhibits a higher sensitivity to more acidic pH values than the cytosolic range.

The other excitation wavelength used to study the pH sensitivity was 440 nm. At this wavelength, where both cis and trans isomers of the chromophore are excited, a dual emission band with green and red peaks at 500 and 625 nm, respectively, is observed (see Fig. 2C). As in the case of the 580 nm excitation wavelength, both emission bands exhibited a decrease in intensity with decreasing pH. However, the rate of decrease differed between the two bands, allowing for a pH-dependent ratiometric analysis of the signals. The difference between the different sensitivities to pH of both bands could be explained because the protonation/deprotonation of residues in the protein affects differently to both isomers leading to a difference in the pH sensitivity.

The value of the ratio, denoted as Ratio R:G, was obtained by dividing the maximum intensity of the red band at 625 nm by the intensity of the green band at 500 nm. This ratio is represented in Fig. 2D. Our data exhibited a maximum ratio value at the lowest pH, followed by a stable ratio value in acidic conditions up to about pH 5.5. Beyond that point, a decrease in the ratio was observed.

3.2. Intracellular calibration and cytosolic pH measurement

One of the most notable applications of genetically encoded probes is in the field of biology. In this context, we investigated their capacity to measure pH levels inside living cells. To begin with, we conducted an intracellular pH calibration using alpha toxin from *Staphylococcus aureus* [33]. At low concentrations, this toxin forms pores in the cytoplasmic membrane, allowing unrestricted diffusion of small molecules between

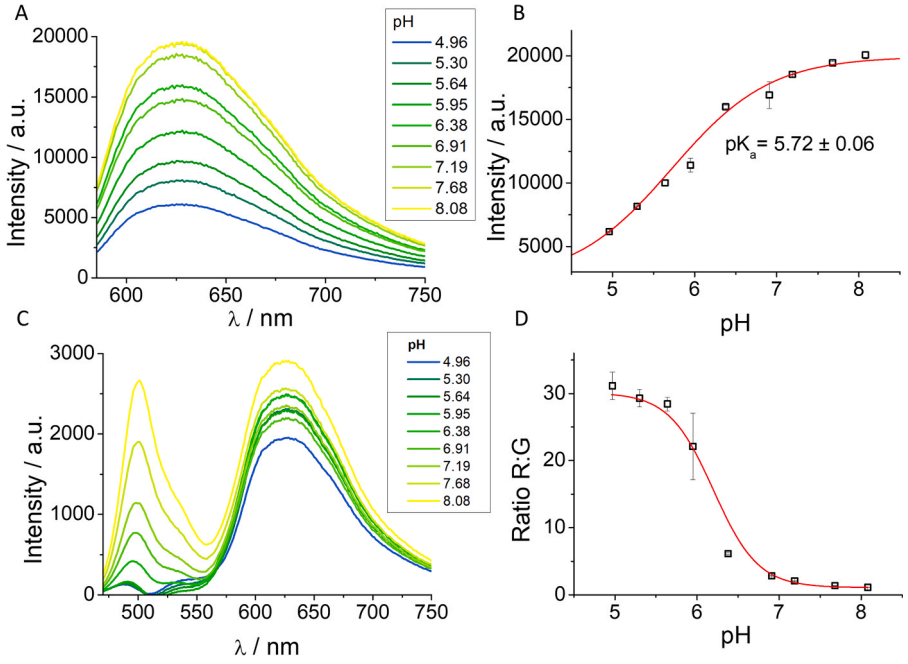

Fig. 2. Study of the dependence of fluorescence emission of mBeRFP D162T with pH. A) Fluorescence emission spectra (λ_{ex}= 580 nm) at different pH values. B) Intensity (λ_{ex} = 580 nm, λ_{em}=625 nm) at different pH values. The curve is the fitting of Eq. 1 to experimental data C) Fluorescence emission spectra (λ_{ex}= 440 nm) at different pH values. D) Ratio values between 625 and 500 nm (Ratio R:G) at different pH values. The line represents a visual aid.

the outside and inside of the cell. To establish a pH gradient, the cells were immersed in buffers with different pH values.

Next, transfected Hela cells expressing the mBeRFP D162T protein were imaged in two different channels: green and red. This enabled us to calculate the ratio R:G. Representative acquired image data are presented in Supporting Information Figure S3, while the corresponding Ratio R:G measurements are displayed in Fig. 3A. We observed a similar pattern compared to the data measured in the solution (see Fig. 2D). Eq. 1 was employed to fit the data, leading to development of a calibration curve that allows the conversion of intracellular Ratio R:G values into pH values. The calibration data are compared with ClopHensor, a genetically encoded pH sensor utilizing E2GFP as pH reporter, as illustrated in Supporting Information, Figure S4A. The probe introduced in this study demonstrates a higher dynamic range than ClopHensor. Further investigations explored la ability to detect pH changes during fasting conditions, showcasing a decrease of the pH compared to control cells (see Supporting Information, Figure S4B). Additionally, experiments studying the photostability of mBeRFP D162T in whole cells and in lysosomes indicate a slightly better stability than mBeRFP and GFP, as shown in Supporting Information, Figure S5. Furthermore, our study on the effect of H_2O_2 on ratio values reveals that ratiometric values remains unaffected within concentrations ranging studied in this work; from 0.1 and 100 μM (see Supporting Information, Figure S6).

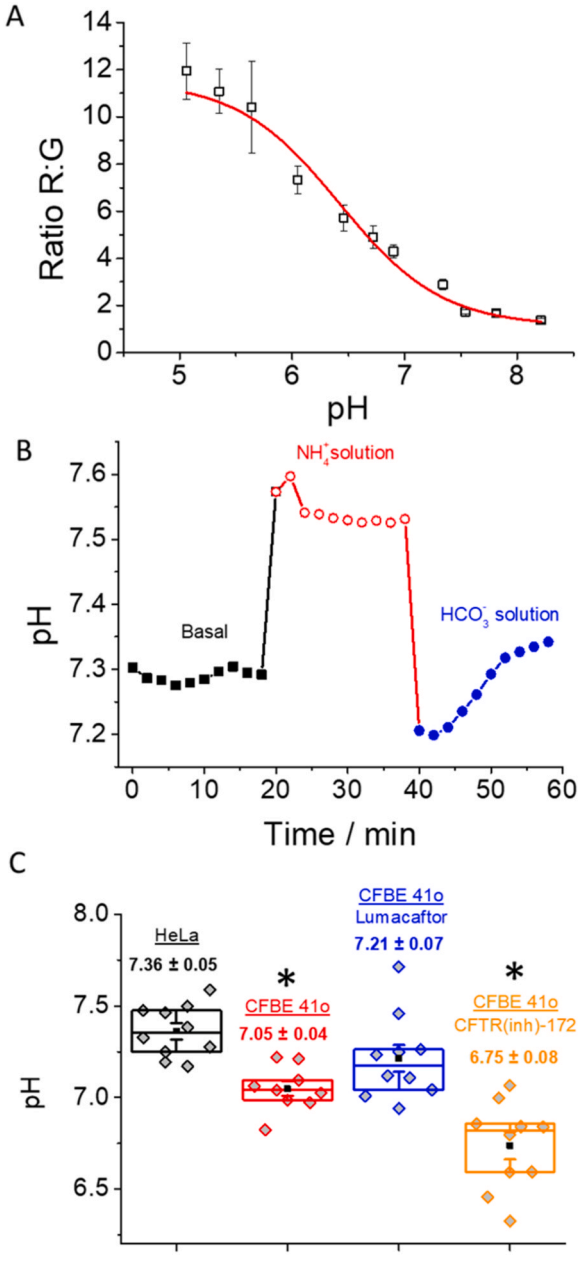

Fig. 3. Intracellular study of the dependence of fluorescence emission of mBeRFP D162T with pH. A) Ratio R:G values obtained from HeLa cells clamped at different pH values. The line represents the fit of the Eq. 1 to the experimental data B) Intracellular pH measurement using ammonium pulse protocol. C) The box and whisker plot representing the pH obtained from HeLa, CFBE41o, CFBE41o with lumacaftor and CFBE41o with CFTR(inh)-172. * $p<0.05$ vs HeLa cells.

Based on our research outcomes, mBeRFP D162T can be considered as a valuable tool for measuring intracellular pH using the ratio between the two emission bands. The intracellular calibration curve showed in Fig. 3A exhibits a dynamic range spanning from 5.0 to 8.00, with an optimal range between 5.5 and 7.0. This characteristic makes it particularly well-suitable for measuring intracellular acidic environments.

To validate the *in vivo* capability to sense pH of mBeRFP D162T, we conducted a test using a NH_4^+ pulse protocol[34,35]. This protocol involves the incubation with NH_4^+ to induce alkalization of the cytosol, followed by its removal to induce an acidification. The pH was subsequently restored by adding a HCO_3^- solution to the bath. Fig. 3B illustrates the observed changes in the pH within a single cell during these solution alterations. As expected, our probe allowed us a continuous monitorization: The introduction of NH_4^+ resulted in an approximate pH increase of 0.25, while its removal led to a decrease of approximately 0.35. The restoration of the pH was achieved after 10/15 minutes.

To further evaluate the ability to monitor intracellular pH fluxes, and to detect small differences in pH, we transfected the mBeRFP D162T plasmid into two different cell lines: HeLa and CFBE 41o. The CFBE41o cell line is derived from a bronchial epithelial cells obtained from a cystic fibrosis patient who is homozygous for the ΔF508 CFTR mutation. After image acquisition, we calculated the Ratio R:G and subsequently converted the obtained data into pH values. Our results revealed pH values of 7.36 ± 0.05 and 7.05 ± 0.04 for HeLa and CFBE 41o cells, respectively. This data is in agreement with other authors measurements, that point out to the fact that the lack of CFTR activity in cystic fibrosis is associated with an impairment in the bicarbonate ions (HCO3−), leading to a cytosol acidification[20]. Furthermore, we conducted evaluations in the CFBE41o cell line in the presence of lumacaftor, a drug known to enhance trafficking of CFTR proteins to the cell surface and enhace bicarbonate transport[25], as well as with CFTR (inh)-172, an inhibitor of CFTR channels[26]. The application of both compounds resulted in notable alterations in the recovered pH values. Lumacaftor led to an increase in intracellular pH, reaching a value of 7.21 ± 0.07. Conversely, the inhibitor caused an elevation in the acidity level of CFBE41o cell line, resulting in a pH value of 6.75 ± 0.08 (see Fig. 3C).

3.3. Lysosomal targeting

Eukaryotic cells have the remarkable feature of segregating the intracellular space into compartments, enabling distinct biochemical processes to occur in separate regions. Each organelle usually maintains a specific pH level, which is associated with the specific biochemical reactions taking place within their compartments. For instance, maintaining the pH within the luminal environment of organelles in the secretory pathway is crucial for the accurate sorting and proteolytic processing of prohormones. Even minor variations in pH can significantly affect prohormone processing[36]. Additionally, determining the pH gradient across the lysosomal membrane provides valuable insights into the cellular processes and functions associated with lysosomes. Monitoring both the internal and external pH, as well as the pH gradient, allows for a comprehensive understanding of the dynamic cellular processes occurring within and around lysosomes.

In order to validate the capability of mBeRFP D162T to detect pH

changes on both the outer (cytosolic) and inner (luminal) surfaces of lysosomes, we present a strategy illustrated in Fig. 3. Our system incorporates the lysosomal-associated membrane protein 1 (LAMP1) domain together with the sequence of the mBeRFP D162T red protein, separated by a linker. As depicted in Fig. 4A, we have employed two different configurations: the first configuration places the LAMP1 domain at the beginning of the fusion protein sequence, while the second configuration positions the LAMP1 domain is at the end of the sequence. This difference in configuration between the two setups, as illustrated in Fig. 4B, results in two distinct effects on the positioning of the mBRFP D162T protein within the lysosomal membrane. In the first configuration (pLAMP1-mBeRFP-D162T), the fluorescent protein is situated on the outer (cytosolic) side of the lysosomal membrane. Conversely, in the second configuration (psignal-mBeRFP-D162T-LAMP1), the fluorescent protein is located within the lysosomal membrane itself facing the lumen of the lysosome. As a consequence, depending on the chosen configuration, the fluorescence of the protein will be influenced by the pH of the environment adjacent to either the outer or inner side of the lysosomal membrane.

In order to demonstrate the organelle targeting of the construct to lysosomes, we transfected HeLa cells with the plasmid psignal-mBeRFP-D162T-LAMP1. Subsequently, we supplemented the cells with the commercial dye LysoTracker™ Green, Mitotracker™ Green or ER Tracker™ Green.

Representative images illustrating the colocalization between the different detection channels are presented in Supporting Information, Figure S7 and the Pearson coefficients obtained are represented in the Fig. 4C. The Pearson values obtained are 0.83 ± 0.06, 0.13 ± 0.05 and 0.20 ± 0.08 for lysosomes, mitochondria and endoplasmic reticulum, respectively. The data demonstrated the excellent overlap between the mBeRFP D162T and lysotracker signals, indicating that the constructed plasmid effectively localized the mBeRFP D162T protein within lysosomes.

Now, to confirm the positioning of mBeRFP D162T within the lysosomal membrane, we conducted an experiment where cells were co-transfected with plasmids sfGFP-Lysosomes-20, that express the GFP protein in the outer face of the lysosome, and psignal-mBeRFP-D162T-LAMP1, that express the mBeRFP D162T in the inner face of the lysosomal membrane. Co-transfected cells expressed mBeRFP-D162T on the inner side and GFP on the outer side of the lysosomal membrane.

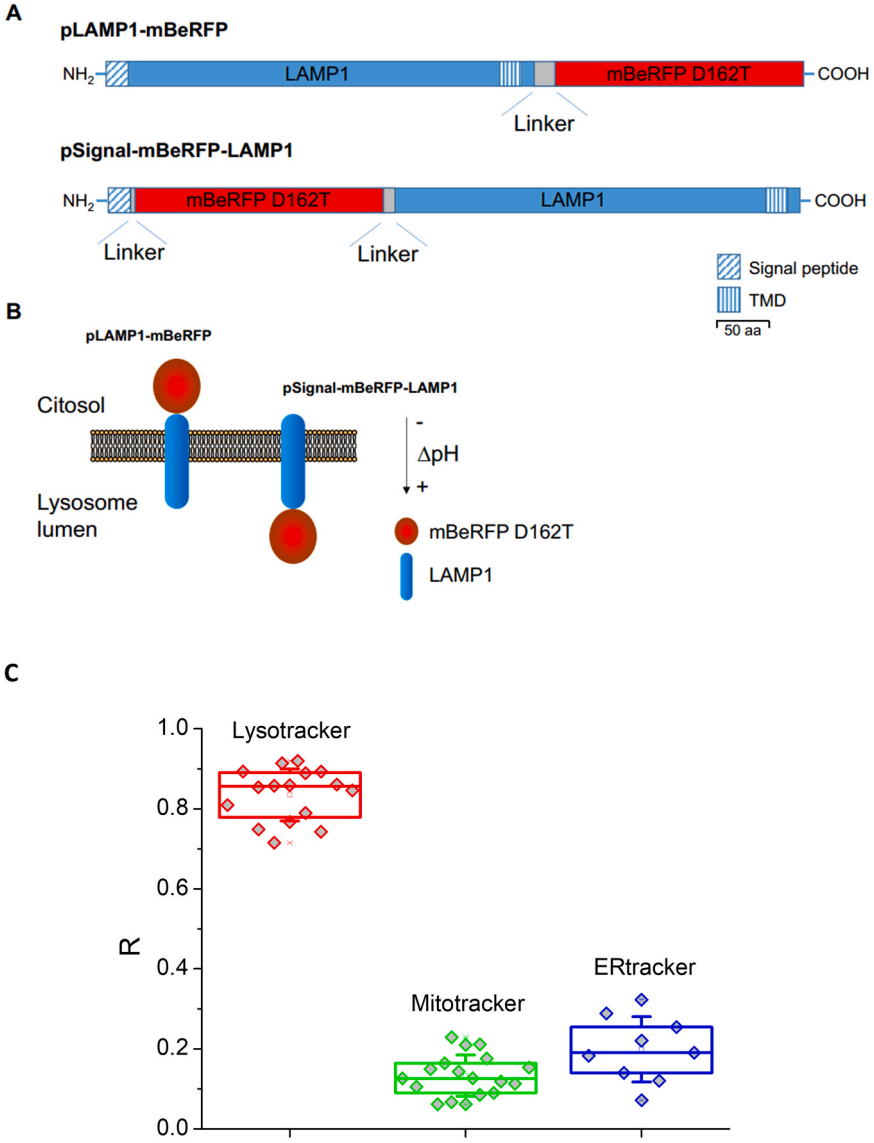

Fig. 4. Scheme of fluorescent proteins used. A) Scheme of pH sensor fusion proteins containing LAMP1, a linker and mBeRFP D162T. B) Schematic representation of the probes with the two different lysosomal locations. Left; citosolyc mBeRFP D162T-LAMP1. Right; luminal mBeRFP D162T-LAMP1. C) Pearson's coefficients calculated with the three biomarkers used, LysoTracker™, MitoTracker™ and ER Tracker™.

Using super-resolution microscopy, we recorded images of lysosomes expressing both fluorescent proteins, as shown in Fig. 5A and Supporting Information Figure S8. The fluorescence of GFP and mBeRFP D162T was captured in two different detection channels: green and red, respectively. In the green channel, GFP-labelled lysosomes on the outer side of the lysosomal membrane are visible. These images show a ring-shaped intensity pattern surrounding the lysosomes. In contrast, the red channel displays a distinct pattern characterized by circular shapes. When these two images are overlapped, it becomes evident that the red fluorescence remains in the central part, while the green fluorescence surrounds it, locating itself in the outermost region. The intensity profiles of both images are depicted in Fig. 5B, where the red channel intensity profile presents a maximum with a Gaussian shape, surrounded by two maxima from the green channel intensity profile. The combination of these fluorescent proteins with advanced imaging techniques allows us to discern the position of these proteins within the lysosome, distinguishing between the interior and exterior regions.

To further confirm the targeting both intra- and extralysosomal regions of mBeRFP-D162T, we calculated the Pearson values using both mBeRFP D162T intra and extralysosomal with lysotracker and sfGFP-Lysosomes-20. These data are shown in Fig. 5C and indicate show a very high Pearson value for the extralysosomal mBeRFP D162T and sfGFP-Lysosomes-20 (0.87 ± 0.05) and intralysosomal mBeRFP D162T and Lysotracker (0.79± 0.03). However, the value decreases for the extralysosomal mBeRFP D162T and Lysotracker (0.59 ± 0.06) and intralysosomal mBeRFP D162T and sfGFP-Lysosomes-20 (0.56 ± 0.08).

These experiments provide the confirmation that the mBeRFP D162T protein can be located either inside or outside the lysosome, anchored to its membrane, depending on its position within the gene sequence. Consequently, the fluorescence signal of the protein will be influenced by the pH value of the inside or outside of the lysosome.

3.4. Lysosomal membrane pH gradient measurement

After confirming the use of both configurations to locate mBeRFP D162T either in the lumen or inner part of the lysosomes, we measured the Ratio R:G of two populations of HeLa cells. One population had mBeRFP D162T located outside the lysosomal membrane, while the other population had mBeRFP D162T situated inside the lysosomal membrane.

As expected, HeLa cells exhibited unique Ratio R:G values between the two populations, depending on whether mBeRFP D162T was measured inside or outside the lysosomes. Acidic conditions inside the lysosomes were characterized by high Ratio R:G values (see Fig. 6A). The measured Ratio R:G was 11.17 ± 1.07, that correspond with a pH value of 4.86 ± 0.48. In contrast to the low Ratio R:G values observed in cells where mBeRFP D162T was located outside the lysosome, here we obtained a ratio R:G of 2.20 ± 0.15, corresponding to a pH value of 7.40 ± 0.07.

To confirm that the signal is indeed dependent on the environmental pH, we employed α-toxin from *Staphilococcus aureus* at high concentrations to permeabilize the lysosomal membrane[37,38]. Following a 30 minutes incubation, we observed a similar Ratio R:G value within the lysosomal lumen, indicating no significant change in the pH (see Supporting Information Figure S9). However, a notable difference was observed in the outer region, where we measured a substantial increase in the Ratio R:G value. This increase corresponds to an acidification of the outer region immediately adjacent to the membrane (see Fig. 6A). These findings are consistent with the hypothesis that the permeabilization of the lysosomal membrane results in the release of hydrogen ions from the inside to the outside of the lysosome, leading to acidification of the area immediately surrounding the membrane. The Ratio R:G values measured in cells treated with α-toxin were 10.40 ±

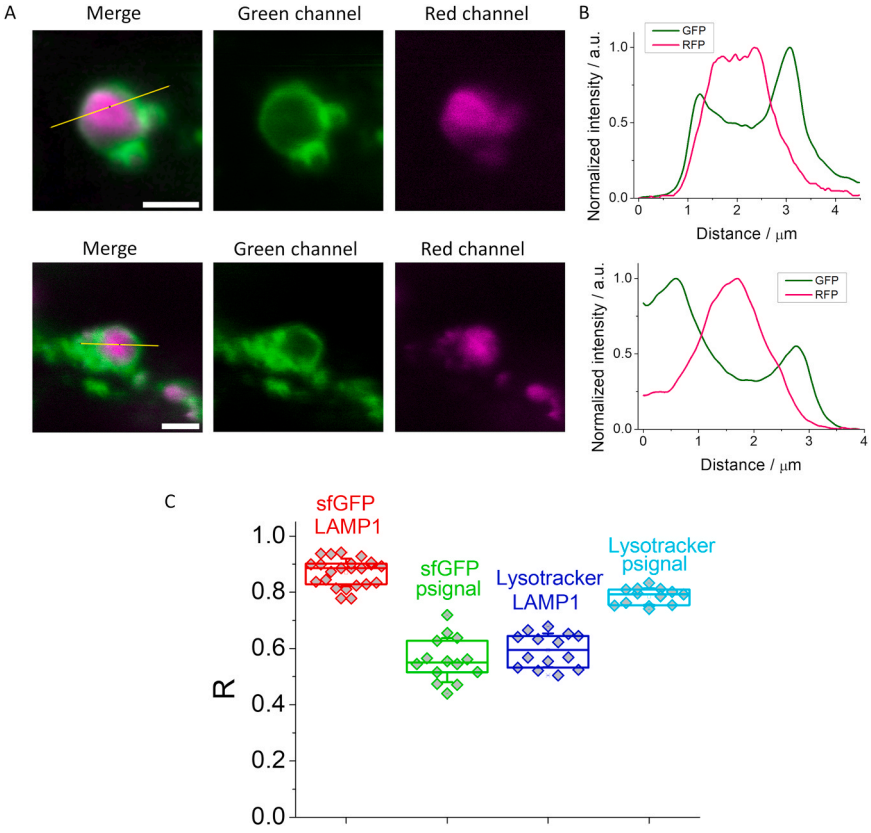

Fig. 5. A) Representative images of lysosomes of merge (left), green (middle) and red (right) channels. Cells were transfected with pSignal-mBeRFP-D162T-LAMP1 (red channel) and sfGFP-Lysosomes-20 (green channel). Scale bars represent 2 μm. B) Intensity plot profile from yellow line in merge channel. C) Pearson's coefficients calculated with, sfGFP-Lysosomes-20, pSignal-mBeRFP-D162T-LAMP1, and LysoTracker™ Green and LAMP1-mBeRFP-D162T.

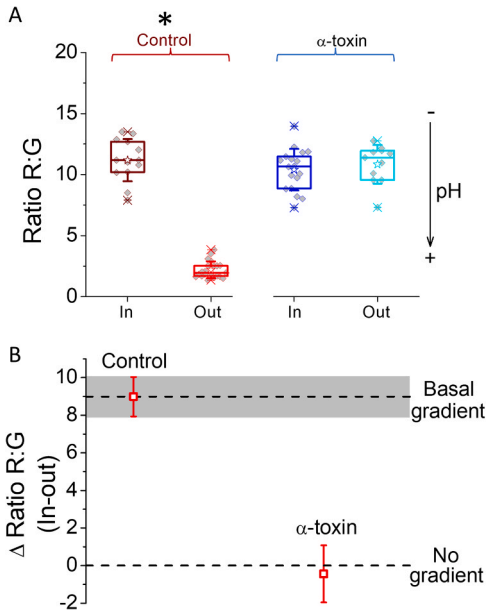

Fig. 6. A) The box and whisker plot representing the Ratio R:G obtained from inside and outside of the lysosomes from different cells at basal condition (left) and after 30 minutes of incubation with α-toxin (right). *p<0.05 between the measurements taken outside and inside the lysosomes. B) Difference of the ratio between inside and outside of the lysosome membrane from control cells and incubated with α-toxin. Upper line represents the basal pH gradient and shadowed rectangle represents the SE. Bottom line represents the absence of pH gradient.

0.40 and 10.84 ± 0.48 for the inner and outer part of the lysosome, respectively. These values correspond with a pH of 5.51 ± 0.16 and 5.25 ± 0.28 in the respective regions.

Interestingly, our system is capable to measure the pH difference (ΔpH, defined as $pH_{in}-pH_{out}$) across the lysosomal membrane by comparing the difference between the Ratio R:G values(ΔRatio R:G = Ratio $R:G_{in}$ − Ratio $R:G_{out}$). As mentioned, a high ratio corresponds to an acidic pH, while a low ratio corresponds to a basic pH. Therefore, a positive ΔRatio R:G indicates a more acidic interior than the exterior, while a negative ΔRatio R:G indicates a more alkaline interior than the exterior. A null ΔRatio R:G would indicate no differences in pH between the interior and exterior, indicating the absence of a pH gradient across the membrane. In Fig. 6B, we present the basal pH gradient represented as ΔRatio R:G of the control cells. By using the average ratio values recovered from Fig. 6A, we determined a positive ΔRatio R:G of 8.93 ± 1.05 indicating a more acidic interior of the lysosome compared to the exterior. Upon the addition of α-toxin, we observed acidification in the outer part of the membrane while maintaining similar pH values in the interior. However, this led to an almost complete loss of the pH gradient between the inner and outer regions of the lysosome, as indicated by the calculated ΔRatio R:G value of 0.89 ± 1.52. Indeed, the observed result is consistent with the action of α-toxin opening pores in the lysosomal membrane, which leads to a loss of the pH gradient across the membrane. This disruption in the membrane integrity allows hydrogen ions to freely diffuse between the interior and exterior of the lysosome, resulting in similar pH values in both regions.

Indeed, while the current configuration of the sensor does not allow for simultaneous measurement of the interior and exterior pH to directly obtain the pH gradient in a single measurement, it still provides valuable information about the lysosomal membrane pH. By measuring the Ratio R:G values inside and outside the lysosomal membrane separately, it is possible to infer the pH gradient between these two regions. The use of this sensor offers the advantages of fluorescent sensors in measuring membrane potentials. Additionally, the use of genetically encoded probes, as the mBeRFP D162T sensor, allows for targeted localization within specific cellular compartments, such as lysosomes. While there may be limitations in simultaneous pH measurements, the information obtained from this sensor can still provide valuable insights into lysosomal membrane potential dynamics and contribute to our understanding of cellular processes and diseases.

Next, in our study, we investigate the effects of various conditions on lysosomal pH. These conditions included the incubation of cells with bafilomycin, chloroquine, dexamethasone, and fasting, all of which have been reported to cause an increase in lysosomal pH, resulting in a more alkaline interior[39,40]. By monitoring the Ratio R:G values of the probe in both configurations, we could observe the changes in lysosomal pH induced by these conditions. Our results were consistent with the literature findings, as we observed a significant decrease in the Ratio R:G values in cells exposed to bafilomycin, chloroquine, dexamethasone, and fasting respect the control cells (Fig. 7A and Supporting Information S3). This decrease indicated a more alkaline lysosomal interior under these conditions.

These findings highlight the effectiveness of our probe in detecting alterations in lysosomal pH and provide valuable insights into the changes that occur in lysosomal pH under different physiological and experimental conditions.

Following the same approach that we performed previously, we have calculated the ΔRatio R:G to visualize the pH gradient between the inner and outer part of the lysosomal membrane (Fig. 7B). In control cells, a clear pH gradient was observed, with a positive ΔRatio R:G indicating a more acidic interior than the exterior of the lysosomes. This gradient is in agreement with previous findings presented in Fig. 6 and reflects the normal physiological state of lysosomes in healthy cells. The preservation of the pH gradient in control cells validates the reliability and reproducibility of the probe's measurements. It also reinforces the accuracy of the pH measurements and the capability of the probe to

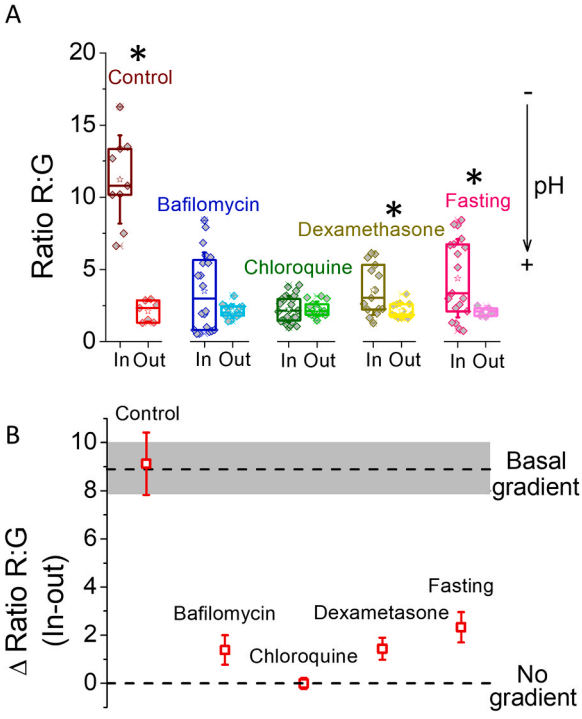

Fig. 7. A) The box and whisker plot representing the Ratio R:G obtained from inside and outside of the lysosomes from different cells at different conditions. *p<0.05 between the measurements taken outside and inside the lysosomes. B) Difference of the ratio between inside and outside of the lysosome membrane at different conditions. Up Line represents the basal pH gradient obtained from control cells and shadowed rectangle represents the SE in Fig. 6. Bottom line represents the absence of pH gradient.

distinguish between the inner and outer parts of the lysosomal membrane.

However, the addition of bafilomycin, dexamethasone, and fasting resulted in a notable decrease in the ΔpH, indicating a loss of the pH gradient across the lysosomal membrane. As we previously described, these conditions led to a more alkaline pH within the lysosomes, resulting in a reduced difference between the inner and outer pH values. The loss of the ΔpH was particularly pronounced with chloroquine, where pH gradient disappeared. Bafilomycin and dexamethasone maintained a slight ΔpH, and fasting exhibited a slight greater ΔpH compared to the other conditions. Despite these variations, the loss of the pH gradient was significant in all cases.

These findings highlight the sensitivity of the mBeRFP D162T probe in detecting changes in lysosomal pH and its potential to provide valuable insights into lysosomal dynamics under various physiological and experimental conditions. The probe's ability to detect alterations in pH and pH gradients can be a valuable tool in understanding lysosomal function and its implications in various cellular processes. By understanding how lysosomal pH is influenced by various factors, we can gain deeper insights into the role of lysosomes in cellular processes and disease mechanisms. The loss of the pH gradient could have important implications for lysosomal function and cellular processes that rely on pH gradients across organelle membranes.

Impairment of the lysosomal pH gradient is observed in various diseases, including CF. In CF there is a defect in lysosomal acidification due to an impaired function of CFTR[21,24], which normally facilitates the influx of chloride ions into the lumen. The most frequent mutation in CFTR producing CF is F508del mutation and is translated into a non-properly folded protein that cannot correctly anchor to the plasma membrane, has a reduced stability and therefore mediates a significantly decreased chloride flux in the cell[41]. CFTR is also responsible for transporting, facilitating the transport of glutathione (GSH) and thiocyanate ions (SCN−), playing a role in immune cell function, and participating in lipid metabolism[20].

The role of CFTR maintaining the acidification of lysosomal compartments in CF cells has been a topic of ongoing of debate[42]. However, recent studies have proposed a model in which CFTR primarily contributes to the acidification of lysosomes. This model supports the notion that CFTR is crucial for the acidification of lysosomes[43].This impairment inhibits the access of electrogenic H+ ions into the lysosomes, leading to an alkalization of the lysosomal interior[44].

Understanding the mechanisms that regulate lysosomal pH and how they are disrupted in diseases like cystic fibrosis is crucial for developing potential therapeutic strategies. Restoring proper lysosomal pH can help maintain normal cellular functions, including the degradation of cellular waste and pathogenic materials, and may offer new avenues for treating lysosomal storage disorders and other diseases associated with lysosomal dysfunction.

Indeed, it is not only important to measure the internal lysosomal pH but also the pH in the surrounding environment of these organelles. In our study, we applied the same approach to determine the intracellular and extracellular pH in cystic fibrosis bronchial CFBE41o cells. In these cells, we observed a loss of acidification in the interior of the lysosomes, as evidenced by the Ratio R:G values being similar to those measured in the extracellular environment (see Fig. 8A and Supporting Information Figure S10). This finding is consistent with the impaired CFTR function observed in cystic fibrosis, which leads to a defective acidification process within the lysosomes[44]. The CFTR-mediated chloride influx, which is responsible for maintaining the proper acidic environment, is compromised in these cells, resulting in an alkalization of the lysosomal interior. The Ratio R:G recovered was 2.13 ± 0.26 and 2.13 ± 0.18 for the inner and outer membrane of lysosomes. These values correspond with pH values of 7.44 ± 0.14 and 7.43 ± 0.10.

Next, we explored the effects of the drug Lumacaftor, which aims to restore functioning CFTR by increasing the trafficking of CFTR proteins to the outer cell membrane[45,46]. We observed a partial restoration of

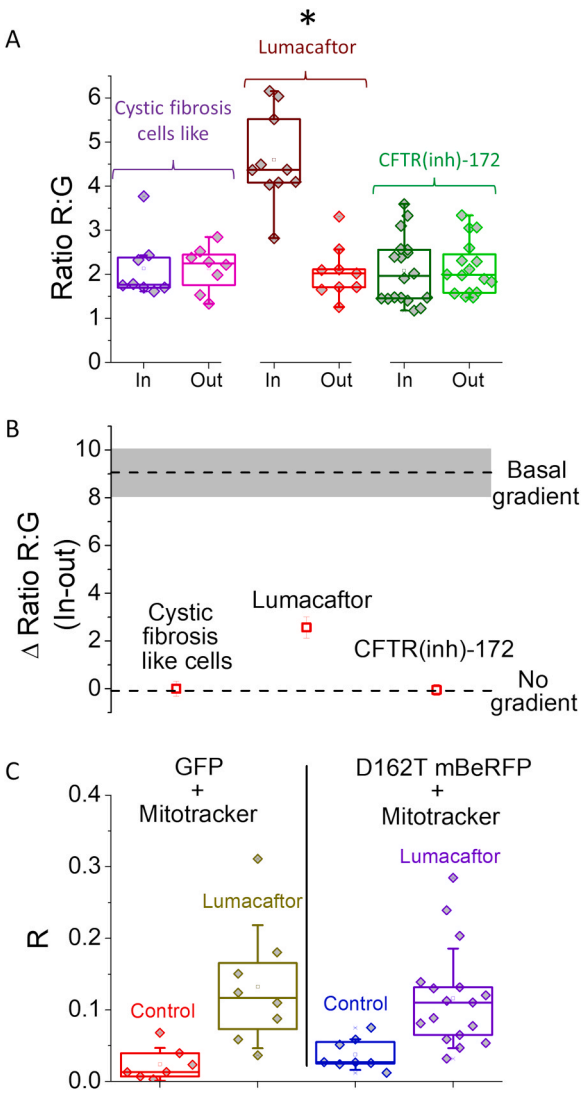

Fig. 8. A) The box and whisker plot representing the Ratio R:G obtained from inside and outside of the lysosomes from different Cystic fibrosis cells like at basal condition and after 30 minutes of incubation with lumacaftor. *p<0.05 between the measurements taken outside and inside the lysosomes. B) Difference of the ratio between inside and outside of the lysosome membrane from Cystic fibrosis cells like and incubated with lumacaftor. Line represents the absence of pH gradient. C) Pearson's coefficients calculated with, sfGFP-Lysosomes-20 (GFP) with MitoTracker™ Far Red and pSignal-mBeRFP-D162T-LAMP1 with MitoTracker™ Far Red.

lysosomal acidification upon treatment with lumacaftor. The Ratio R:G values measured was 4.60 ± 0.32 and 2.04 ± 0.20 for the inner and outer membrane of lysosomes, respectively. These values correspond with pH values of 6.75 ± 0.06 and 7.48 ± 0.12. Additionally, to further investigate the impact of CFTR impairment, we used CFTR(inh)-172, an inhibitor of CFTR activity. In contrast to the results obtained with Lumacaftor, the use of CFTR(inh)-172 led to a slight modification in the opposite direction, resulting in an additional alkalization of the lysosomal interior. The Ratio R:G recovered was 2.08 ± 0.18 and 2.13 ± 0.15 for the inner and outer membrane of lysosomes. These values correspond with 7.46 ± 0.10 and 7.43 ± 0.08, respectively. These findings indicate that Lumacaftor may partially restore lysosomal acidification by improving CFTR function and increasing the trafficking of CFTR proteins to the cell membrane. On the other hand, the use of CFTR (inh)-172 exacerbates the lysosomal alkalization, suggesting the critical role of CFTR in maintaining proper lysosomal pH levels. Fig. 8B shows

the ΔRatio R:G, which visualizes the pH gradient in these conditions. In CFBE41o cells, we observed a complete absence of pH gradient across the membrane, which is partially restored upon the addition of the drug Lumacaftor. Hoiwever, when using CFTR(inh)-172, the pH gradient remains null across the lysosomal membrane.

From the data obtained in Hela and Cystic fibrosis cells, our system based on the mBeRFP D162T protein has proven to be a valuable tool for measuring intralysosomal or extralysosomal pH in live cells. The dual emission band of this protein allow us to obtain pH information from both regions with high accuracy. However, the current two-step experiment for measuring the pH gradient across the lysosomal membrane may be considered a limitation in terms of efficiency and time-consuming procedures. To address this limitation, we envision potential improvements in future approaches. One strategy to overcome this limitation is the implementation of bicistronic systems and molecular switches. This genetic modification could allow simultaneous and independent measure of intralysosomal and extralysosomal pH within the same population of cells. This approach would significantly streamline the experimental process and reduce the need for separate samples.

Cystic fibrosis cells show enhanced mitochondrial damage associated with a diminished clearance through mitophagy is associated with a mito-inflammatory phenotype [47]. This situation can be reverted at least partially using CFTR trafficking enhancers as lumacaftor and restoring mitophagy [48]. Since classic methods to measure mitophagy are based on the assessment of the fusion of mitochondria to lysosomes using labeled organelles [28], we have made a preliminary study of the feasibility of the use of our pSignal-mBeRFP-D162T -LAMP1 plasmid compared with the pGFP-LC3 standard plasmid. For that, CFBE41o were transfected either with pGFP-LC3 or pSignal-mBeRFP-D162T -LAMP1 and then labeled with miTotracker deep red FM and mitophagy was assessed by colocalization of the signals. Our results (Fig. 8C) show that by using either pGFP-LC3 or pSignal-mBeRFP-D162T -LAMP1 plasmid mitophagy can be measured in the CF cells and as expected the pre-incubation with lumacaftor was able to increase mitophagy.

In conclusion, our study has presented a novel approach to measure cytosolic, intralysosomal and extralysosomal pH using the mBeRFP D162T protein, with its two emission bands providing precise information about the acidity in both cellular regions. We have demonstrated the effectiveness of this system in evaluating cytosol and lysosomal pH under various experimental and physiological conditions, including pH reduction induced by agents like bafilomycin and dexamethasone, as well as partial restoration with lumacaftor. Furthermore, we confirmed the complete loss of lysosomal pH gradient in CFBE41o cells, a cystic fibrosis model, due to impaired intralysosomal acidification. Our approach reliably measured the pH gradient between the lysosomal interior and exterior, opening new avenues for studying lysosome-related diseases and potential therapeutic developments.

CRediT authorship contribution statement

Jose Manuel Paredes: Writing – review & editing, Writing – original draft, Project administration, Methodology, Investigation, Funding acquisition, Formal analysis, Data curation, Conceptualization. **María Dolores Giron:** Writing – review & editing, Writing – original draft, Project administration, Methodology, Investigation, Funding acquisition, Formal analysis, Data curation, Conceptualization. **Rafael Salto:** Writing – review & editing, Writing – original draft, Resources, Project administration, Methodology, Investigation, Funding acquisition, Formal analysis, Data curation, Conceptualization.

Declaration of Competing Interest

The authors declare that they have no known competing financial interests or personal relationships that could have appeared to influence the work reported in this paper.

Data Availability

Data will be made available on request.

Acknowledgment

Research grant Junta de Andalucía A-CTS-186-UGR20 and A-FQM-230-UGR20, co-financed by FEDER funds. Spanish Ministry of Science and Innovation (AEI, Spain, PID2020–113059GB-C21. J.M.P. thank "Microproyectos" grant for UEQ.

Author contributions

The manuscript was written through contributions of all authors. All authors have given approval to the final version of the manuscript.

Notes

The authors declare no competing financial interest.

Appendix A. Supporting information

Supplementary data associated with this article can be found in the online version at doi:10.1016/j.snb.2024.135673.

References

[1] D.M. Chudakov, M.V. Matz, S. Lukyanov, K.A. Lukyanov, Fluorescent proteins and their applications in imaging living cells and tissues, Physiol. Rev. 90 (3) (2010) 1103–1163.
[2] J.R. Enterina, L.S. Wu, R.E. Campbell, Emerging fluorescent protein technologies, Curr. Opin. Chem. Biol. 27 (2015) 10–17.
[3] V.I. Martynov, A.A. Pakhomov, I.E. Deyev, A.G. Petrenko, Genetically encoded fluorescent indicators for live cell pH imaging, Biochim. Et. Biophys. Acta-Gen. Subj. 1862 (12) (2018) 2924–2939.
[4] H. Shinoda, M. Shannon, T. Nagai, Fluorescent Proteins for Investigating Biological Events in Acidic Environments, Int J. Mol. Sci. 19 (6) (2018) 1548.
[5] A. Esposito, M. Gralle, M.A.C. Dani, D. Lange, F.S. Wouters, pHlameleons: A Family of FRET-Based Protein Sensors for Quantitative pH Imaging, Biochemistry 47 (49) (2008) 13115–13126.
[6] D.B. Betolngar, M. Erard, H. Pasquier, Y. Bousmah, A. Diop-Sy, E. Guiot, et al., pH sensitivity of FRET reporters based on cyan and yellow fluorescent proteins, Anal. Bioanal. Chem. 407 (14) (2015) 4183–4193.
[7] L. Karsten, L. Goett-Zink, J. Schmitz, R. Hoffrogge, A. Grunberger, T. Kottke, et al., Genetically Encoded Ratiometric pH Sensors for the Measurement of Intra- and Extracellular pH and Internalization Rates, Biosens. -Basel 12 (5) (2022) 271.
[8] J.M. Paredes, A.I. Idilli, L. Mariotti, G. Losi, L.R. Arslanbaeva, S.S. Sato, et al., Synchronous Bioimaging of Intracellular pH and Chloride Based on LSS Fluorescent Protein, ACS Chem. Biol. 11 (6) (2016) 1652–1660.
[9] G. Miesenbock, D.A. De Angelis, J.E. Rothman, Visualizing secretion and synaptic transmission with pH-sensitive green fluorescent proteins, Nature 394 (6689) (1998) 192–195.
[10] Y.G. Ermakova, V.V. Pak, Y.A. Bogdanova, A.A. Kotlobay, I.V. Yampolsky, A. G. Shokhina, et al., SypHer3s: a genetically encoded fluorescent ratiometric probe with enhanced brightness and an improved dynamic range, Chem. Commun. 54 (23) (2018) 2898–2901.
[11] R. Bizzarri, C. Arcangeli, D. Arosio, F. Ricci, P. Faraci, F. Cardarelli, et al., Development of a novel GFP-based ratiometric excitation and emission pH indicator for intracellular studies, Biophys. J. 90 (9) (2006) 3300–3314.
[12] G.T. Hanson, T.B. McAnaney, E.S. Park, M.E.P. Rendell, D.K. Yarbrough, S.Y. Chu, et al., Green fluorescent protein variants as ratiometric dual emission pH sensors. 1. Structural characterization and preliminary application, Biochemistry 41 (52) (2002) 15477–15488.
[13] M. Bencina, Illumination of the Spatial Order of Intracellular pH by Genetically Encoded pH-Sensitive Sensors, Sensors 13 (12) (2013) 16736–16758.
[14] S. Zhang, H.W. Ai, A general strategy to red-shift green fluorescent protein-based biosensors, Nat. Chem. Biol. 16 (12) (2020) 1434–1439.
[15] F.V. Subach, K.D. Piatkevich, V.V. Verkhusha, Directed molecular evolution to design advanced red fluorescent proteins, Nat. Methods 8 (12) (2011) 1019–1026.
[16] M. Tantama, Y.P. Hung, G. Yellen, Imaging Intracellular pH in Live Cells with a Genetically Encoded Red Fluorescent Protein Sensor, J. Am. Chem. Soc. 133 (26) (2011) 10034–10037.
[17] J. Yang, L. Wang, F. Yang, H.M. Luo, L.L. Xu, J.L. Lu, et al., mBeRFP, an Improved Large Stokes Shift Red Fluorescent Protein, PLoS One 8 (6) (2013) e64849.
[18] R. Salto, M.D. Giron, V. Puente-Muñoz, J.D. Vilchez, L. Espinar-Barranco, J. Valverde-Pozo, et al., New Red-Emitting Chloride-Sensitive Fluorescent Protein with Biological Uses, ACS Sens. 6 (7) (2021) 2563–2573.

[19] F.Y. Liu, Z. Zhang, L. Csanady, D.C. Gadsby, J. Chen, Molecular Structure of the Human CFTR Ion Channel, Cell 169 (1) (2017) 85–95.e8.
[20] L.S. Hanssens, J. Duchateau, G.J. Casimir, CFTR Protein: Not Just a Chloride Channel? Cells 10 (11) (2021) 2844.
[21] J. Barasch, B. Kiss, A. Prince, L. Saiman, D. Gruenert, Q. Alawqati, Defective Acidification of Intracellular Organelles in Cystic-Fibrosis, Nature 352 (6330) (1991) 70–73.
[22] J. Liu, W.N. Lu, S. Guha, G.C. Baltazar, E.E. Coffey, A.M. Laties, et al., Cystic fibrosis transmembrane conductance regulator contributes to reacidification of alkalinized lysosomes in RPE cells, Am. J. Physiol. -Cell Physiol. 303 (2) (2012) C160–C169.
[23] A. Di, M.E. Brown, L.V. Deriy, C.Y. Li, F.L. Szeto, Y.M. Chen, et al., CFTR regulates phagosome acidification in macrophages and alters bactericidal activity, Nat. Cell Biol. 8 (9) (2006) 933–U52.
[24] A. Lukasiak, M. Zajac, The Distribution and Role of the CFTR Protein in the Intracellular Compartments, Membranes 11 (11) (2021) 804.
[25] L. Ferrera, D. Baroni, O. Moran, Lumacaftor-rescued F508del-CFTR has a modified bicarbonate permeability, J. Cyst. Fibros. 18 (5) (2019) 602–605.
[26] E. Caci, A. Caputo, A. Hinzpeter, N. Arous, P. Fanen, N. Sonawane, et al., Evidence for direct CFTR inhibition by CFTR(inh)-172 based on Arg347 mutagenesis. Biochem J. 413 (1) (2008) 135–142.
[27] M. Kucinska, M.-D. Giron, H. Piotrowska, N. Lisiak, W.H. Granig, F.-J. Lopez-Jaramillo, et al., Novel Promising Estrogenic Receptor Modulators: Cytotoxic and Estrogenic Activity of Benzanilides and Dithiobenzanilides, PLoS One 11 (1) (2016) e0145615.
[28] Chen L., Ma K., Han J., Chen Q., Zhu Y. Monitoring Mitophagy in Mammalian Cells. In: Galluzzi L, Pedro J, Kroemer G, editors. Molecular Characterization of Autophagic Responses, Pt B 2017. p. 187-208.
[29] J. Schindelin, I. Arganda-Carreras, E. Frise, V. Kaynig, M. Longair, T. Pietzsch, et al., Fiji: an open-source platform for biological-image analysis, Nat. Methods 9 (7) (2012) 676–682.
[30] S. Pletnev, D. Shcherbo, D.M. Chudakov, N. Pletneva, E.M. Merzlyak, A. Wlodawer, et al., A Crystallographic Study of Bright Far-Red Fluorescent Protein mKate Reveals pH-induced cis-trans Isomerization of the Chromophore, J. Biol. Chem. 283 (43) (2008) 28980–28987.
[31] N.V. Pletneva, V.Z. Pletnev, I.I. Shemiakina, D.M. Chudakov, I. Artemyev, A. Wlodawer, et al., Crystallographic study of red fluorescent protein eqFP578 and its far-red variant Katushka reveals opposite pH-induced isomerization of chromophore, Protein Sci. 20 (7) (2011) 1265–1274.
[32] Q. Wang, L.J. Byrnes, B. Shui, U.F. Rohrig, A. Singh, D.M. Chudakov, et al., Molecular Mechanism of a Green-Shifted, pH-Dependent Red Fluorescent Protein mKate Variant, PLoS One 6 (8) (2011) e23513.
[33] J.M. Paredes, M.D. Giron, M.J. Ruedas-Rama, A. Orte, L. Crovetto, E.M. Talavera, et al., Real-Time Phosphate Sensing in Living Cells using Fluorescence Lifetime Imaging Microscopy (FLIM), J. Phys. Chem. B 117 (27) (2013) 8143–8149.
[34] M. Fiore, C. Picco, O. Moran, Correctors modify the bicarbonate permeability of F508del-CFTR, Sci. Rep. 10 (1) (2020) 8440.
[35] D.B. Kintner, G. Su, B. Lenart, A.J. Ballard, J.W. Meyer, L.L. Ng, et al., Increased tolerance to oxygen and glucose deprivation in astrocytes from Na+/H+ exchanger isoform 1 null mice, Am. J. Physiol. -Cell Physiol. 287 (1) (2004) C12–C21.
[36] W.K. Schmidt, H.P.H. Moore, Ionic Milieu Controls the Compartment-Specific Activation of Proopiomelanocortin Processing in ATT-20 Cells, Mol. Biol. Cell 6 (10) (1995) 1271–1285.
[37] A.W. Bernheimer, L.L. Schwartz, LYSOSOMAL DISRUPTION BY BACTERIAL TOXINS, J. Bacteriol. 87 (5) (1964) 1100–1104.
[38] J. Ma, E. Gulbins, M.J. Edwards, C.C. Caldwell, M. Fraunholz, K.A. Becker, Staphylococcus aureus alpha-Toxin Induces Inflammatory Cytokines via Lysosomal Acid Sphingomyelinase and Ceramides, Cell Physiol. Biochem 43 (6) (2017) 2170–2184.
[39] S.H. Park, J.Y. Hyun, I. Shin, A lysosomal chloride ion-selective fluorescent probe for biological applications, Chem. Sci. 10 (1) (2019) 56–66.
[40] Xu H.X., Ren D.J. Lysosomal Physiology. In: Julius D, editor. Annual Review of Physiology, Vol 772015. p. 57-80.
[41] B. Kleizen, J.F. Hunt, I. Callebaut, T.C. Hwang, I. Sermet-Gaudelus, S. Hafkemeyer, et al., CFTR: New insights into structure and function and implications for modulation by small molecules, J. Cyst. Fibros. 19 (2020) S19–S24.
[42] S.M. Law, S.J. Stanfield, G.R. Hardisty, I. Dransfield, C.J. Campbell, R.D. Gray, Human cystic fibrosis monocyte derived macrophages display no defect in acidification of phagolysosomes when measured by optical nanosensors, J. Cyst. Fibros. 19 (2) (2020) 203–210.
[43] A. Badr, M. Eltobgy, K. Krause, K. Hamilton, S. Estfanous, K.P. Daily, et al., CFTR Modulators Restore Acidification of Autophago-Lysosomes and Bacterial Clearance in Cystic Fibrosis Macrophages, Front. Cell. Infect. Microbiol. 12 (2022) 819554.
[44] P.M. Haggie, A.S. Verkman, Unimpaired Lysosomal Acidification in Respiratory Epithelial Cells in Cystic Fibrosis, J. Biol. Chem. 284 (12) (2009) 7681–7686.
[45] G.J. Connett, Lumacaftor-ivacaftor in the treatment of cystic fibrosis: design, development and place in therapy, Drug Des. Dev. Ther. 13 (2019) 2405–2412.
[46] M.C. Dechecchi, A. Tamanini, G. Cabrini, Molecular basis of cystic fibrosis: from bench to bedside, Ann. Transl. Med. 6 (17) (2018) 334.
[47] S. Patergnani, V.A.M. Vitto, P. Pinton, A. Rimessi, Mitochondrial Stress Responses and "Mito-Inflammation" in Cystic Fibrosis, Front Pharm. 11 (2020) 581114.
[48] C. Braccia, J.A. Christopher, O.M. Crook, L.M. Breckels, R.M.L. Queiroz, N. Liessi, et al., CFTR Rescue by Lumacaftor (VX-809) Induces an Extensive Reorganization of Mitochondria in the Cystic Fibrosis Bronchial Epithelium, Cells 11 (12) (2022) 1938.

Prof. Rafael Salto graduated in Pharmacy in 1985 and obtained the Ph. D. degree in 1989 at the Granada University. He completed his scientific training first as a Fulbright Scholar at the University of California at San Francisco (UCSF) with the Professor Charles S. Craik and later as a postdoctoral fellow with the Professor Juan Luis Ramos at the Spanish Research Council, back in Granada. He is Full Professor at the Department of Biochemistry and Molecular Biology of the School of Pharmacy at the University of Granada (Spain), and head of the "Genetic and Biochemical Regulation of Metabolism (BIO212)" research group that is supported by the regional government (Junta de Andalucía).

Prof. Maria D. Giron is a Full Professor at the Department of Biochemistry and Molecular Biology, University of Granada, Spain. She obtained her PhD in Pharmacy in 1988. Her research interests are mainly related: (i) to the search of new compounds with the ability to target proteins involved in different pathologies such as diabetes, obesity or cancer and (ii) the biological characterization of theranostics compounds of importance in biomedicine.

José M. Paredes graduated in Pharmacy in 2004 and obtained the Ph. D. degree in 2010 at the University of Granada. From 2012–2015, he was a postdoctoral fellow of the Institute of Biophysics (CNR) and Fondazione Bruno Kessler (FBK) in Trento (Italy). Currently, he is Professor at the Department of Physical Chemistry of the Faculty of Pharmacy at the University of Granada (Spain). His research interests include the development of fluorescence sensors for biomedical applications, fluorescence imaging microscopy, photophysics and related fields.